Study on the Optical Properties of Nanowires Using FDTD Method

Xiang Huang[a], Liang Yu[a], Jin-Yang Chu[a], Zhi-Xiang Huang[a*], Xian-Liang Wu[a,b*]
[a]Key Laboratory of Intelligent Computing and Signal Processing, Anhui University, Hefei 230039,China
[b]School of Electronic and Information Engineering, Hefei Normal University, Hefei 230061,China
*Email: zxhuang@ahu.edu.cn, xlwu@ahu.edu.cn

***Abstract*- Finite-difference time-domain studies of a variety of cylinder arrays with nanometer-scale diameters (nanowires) interacting with light are presented. Scattering and absorption cross sections for metallic nanoscale objects can be obtained from such calculation. The method is verified by comparing the analytical results for cylindrical nanowires. Calculate the optical properties of Ag nanowires and study the explicit time-domain behavior of more cylinders.**

***Keywords*- Finite-Difference Time-Domain Method, Absorption Cross Section, Scattering Cross Section, Extinction Cross Section**

I. INTRODUCTION

The finite-difference time-domain (FDTD) method, since its introduction by Yee[1], has been widely used to obtain numerical solutions of Maxwell's equations for a broad range of problems. The applications of FDTD in electrodynamics include antenna and radar design, electronic and photonic circuit design, microwave tomography, cellular and wireless network simulation, mobile phone safety studies, and many more. The method is not limited to electrodynamics and can be used to solve other spatiotemporal partial differential equations such as those occurring in acoustics. The explicit nature of FDTD formulation, its simplicity, accuracy and robustness, together with a well established theoretical framework have contributed to a seemingly unending popularity of the method.

Nanowires, unlike other low-dimensional systems, have two quantum-confined directions but one unconfined direction available for electrical conduction. At the same time, owing to their unique density of electronic states, in the limit of small diameters, nanowires are expected to exhibit significant different optical, electrical, and magnetic properties. Here we show how finite-difference time-domain FDTD calculations can be used to study light interacting with arrays of cylinders with nanoscale diameters, and we carry out a variety of studies of various configurations. The cylinders can be viewed as metallic nanowires and exhibit optical behavior similar to metal nanoparticles (MNP's). In particular, surface plasmon polarizations (SPP's), resonance interactions of light with electronic charge density near the metal surface, [2] can play an important role.

Section II outlines our theoretical and computational methods. Section III presents cross-section results for Ag cylinders. Section Ⅳ concludes the paper.

II. THEORETICAL AND NUMERICAL CALCULATION MODEL

A. FDTD Algorithm of Metal Nanowires

The interaction of light with matter in the classical continuum limit is described by Maxwell's equations. Frequency-domain solutions to Maxwell's equations for light interacting with materials are constructed by allowing spatial (x,y,z) and possibly light frequency variation in the dielectric constant ε. In a region of space (x,y,z) occupied by a metal, ε can be complex valued and frequency dependent: $\varepsilon = \varepsilon_0 \varepsilon_r(\omega)$,where ε_0 is the permittivity of free space. In classical electrodynamics, materials are described through a dielectric function ε that relates the electric displacement field **D** to the electric field **E** at a given frequency of light ω

$$\mathbf{D}(\omega) = \varepsilon_0 \varepsilon_r(\omega)\mathbf{E}(\omega) \tag{1}$$

The dielectric function of a metal like Ag is well-described in the classical continuum limit by three separate components,

$$\varepsilon_r(\omega) = \varepsilon_\infty + \varepsilon_{inter}(\omega) + \varepsilon_{intra}(\omega) \tag{2}$$

with, ε_∞ , a contribution from *d*-band to *sp*-band (conduction band) inter band electron transitions, $\varepsilon_{inter}(\omega)$, and a contribution due to *sp*-band electron excitations, $\varepsilon_{intra}(\omega)$.

$\varepsilon_{inter}(\omega)$ can be physically described using a multipole Lorentz oscillator model[3] .

$$\varepsilon_{inter}(\omega) = \sum_j \frac{\Delta\varepsilon_{Lj}\omega_{Lj}^2}{\omega_{Lj}^2 - \omega\left(\omega + i2\delta_{Lj}\right)} \tag{3}$$

where *j* is an index labeling the individual *d*-band to *sp*-band electron transitions occurring at ω_{Lj} . In order to fit the two interband transitions in Ag at designed band of frequencies[4],we choose $j = 2$.

$\varepsilon_{intra}(\omega)$ is responsible for the plasmonic optical response of metals. It can be described by the hydrodynamic Drude model[5].

$$\varepsilon_{intra}(\omega) = -\frac{\omega_D^2}{\omega\left(\omega + i\gamma\right)} \tag{4}$$

where ω_D is the plasma frequency, γ is the collision frequency.

Insert Eqs. (1) and (2) into the Ampere law for a time-harmonic field, lead to

$$-i\omega\varepsilon_0\varepsilon_\infty\mathbf{E}(\omega) + \sum_j \mathbf{J}_{Lj}(\omega) + \mathbf{J}_{HD}(\omega) = i\mathbf{k}\times\mathbf{H}(\omega) \tag{5}$$

with

$$\mathbf{J}_{Lj}(\omega) = -i\omega\varepsilon_0 \frac{\Delta\varepsilon_{Lj}\omega_{Lj}^2}{\omega_{Lj}^2 - \omega(\omega + i2\delta_{Lj})}\mathbf{E}(\omega) \quad (6)$$

$$\mathbf{J}_{HD}(\omega) = i\omega\varepsilon_0 \frac{\omega_D^2}{\omega(\omega + i\gamma)}\mathbf{E}(\omega) \quad (7)$$

Conveniently exploiting the differentiation theorem for the Fourier transform, we perform an inverse Fourier transformation of each term of (6) and (7). Thus, we can get

$$\frac{\partial^2}{\partial t^2}\mathbf{J}_{Lj}(t) + 2\delta_{Lj}\frac{\partial}{\partial t}\mathbf{J}_{Lj}(t) + \omega_{Lj}^2\mathbf{J}_{Lj}(t) = \varepsilon_0\Delta\varepsilon_{Lj}\omega_{Lj}^2\frac{\partial}{\partial t}\mathbf{E}(t) \quad (8)$$

$$\frac{\partial^2}{\partial t^2}\mathbf{J}_{\mathrm{HD}}(t) + \gamma\frac{\partial}{\partial t}\mathbf{J}_{\mathrm{HD}}(t) = \varepsilon_0\omega_D^2\frac{\partial}{\partial t}\mathbf{E}(t) \quad (9)$$

Eqs. (8) and (9) can be solved self-consistent with Maxwell's equations. The inverse Fourier-transformed form of Eq.(5) is

$$\varepsilon_0\varepsilon_\infty\frac{\partial}{\partial t}\mathbf{E}(t) + \sum_j \mathbf{J}_{Lj}(t) + \mathbf{J}_{HD}(t) = \nabla\times\mathbf{H}(t) \quad (10)$$

Specializing to the transverse electric (*TE*) case with cylindrical symmetry, we drop the z coordinate in all equations and deal with just three of the six field components, E_x,E_y, and H_z.

B. Cross-Section Formulas

The optical properties of most of the nanostructures are determined from intensity profiles of the electromagnetic fields, or from their optical cross sections[6]. A cross section is the effective area that governs the probability of some scattering or absorption event.

We use a simple, direct procedure, which is both feasible and sufficiently accurate for our purposes, to estimate cross sections[7]. From the above description, we can get real-valued time-dependent electric-field and magnetic-field vectors $\mathbf{E}(t) = \mathbf{E}(x,y,z,t)$ and $\mathbf{H}(t) = \mathbf{H}(x,y,z,t)$, consistent with an appropriate initial pulse or a source, and scattering off one or more particles, the complex, frequency-resolved total fields are

$$\mathbf{E}(\omega) = \int_0^\infty dt\exp(i\omega t)\mathbf{E}(t) \quad (11)$$

$$\mathbf{H}(\omega) = \int_0^\infty dt\exp(i\omega t)\mathbf{H}(t) \quad (12)$$

A comparable calculation, but we must know the incident time-dependent fields $\mathbf{E}_{inc}(t)$ and $\mathbf{H}_{inc}(t)$, with the frequency-resolved incident fields

$$\mathbf{E}_{inc}(\omega) = \int_0^\infty dt\exp(i\omega t)\mathbf{E}_{inc}(t) \quad (13)$$

$$\mathbf{H}_{inc}(\omega) = \int_0^\infty dt\exp(i\omega t)\mathbf{H}_{inc}(t) \quad (14)$$

The scattered fields are then given by

$$\mathbf{E}_{sca}(\omega) = \mathbf{E}(\omega) - \mathbf{E}_{inc}(\omega) \quad (15)$$

$$\mathbf{H}_{sca}(\omega) = \mathbf{H}(\omega) - \mathbf{H}_{inc}(\omega) \quad (16)$$

Cross sections means per unit length of the cylinder axis, which therefore have units of length as opposed to length, are calculated. The corresponding scattering cross section is

$$\sigma_{sca}(\omega) = \frac{P_{sca}(\omega)}{I_{inc}(\omega)} \quad (17)$$

where $P_{sca}(\omega)$ is the absorbed power per unit area, and $I_{inc}(\omega)$ is the magnitude of the incident power. In terms of the (time-averaged) Poynting vector associated with the scattered fields, $\mathbf{S}_{sca}$, and employing cylindrical coordinates (r,φ,z),

$$P_{sca}(\omega) = r_\infty\int_0^{2\pi} d\varphi\mathbf{S}_{sca}(\omega)\cdot\mathbf{r}|_{r=r_\infty} \quad (18)$$

Where the path of integration is along a circle of large radius r_∞ surrounding the cylinder for any value of z, and

$$\mathbf{S}_{sca}(\omega) = \frac{1}{2}\mathrm{Re}\left[\mathbf{E}_{sca}(\omega)\times\mathbf{H}_{sca}^*(\omega)\right] \quad (19)$$

The absorption cross section is given by

$$\sigma_{abs}(\omega) = \frac{P_{abs}(\omega)}{I_{inc}(\omega)} \quad (20)$$

with

$$P_{abs}(\omega) = r_\infty\int_0^{2\pi} d\varphi\mathbf{S}_{abs}(\omega)\cdot\mathbf{r}|_{r=r_\infty} \quad (21)$$

$$\mathbf{S}_{abs}(\omega) = \frac{1}{2}\mathrm{Re}\left[\mathbf{E}(\omega)\times\mathbf{H}(\omega)^*\right] \quad (22)$$

The extinction cross section is a sum of the two,

$$\sigma_{ext}(\omega) = \sigma_{sca}(\omega) + \sigma_{abs}(\omega) \quad (23)$$

A useful check of the numerical calculations is to determine the extinction cross section directly via the formula

$$\sigma_{ext}(\omega) = \frac{P_{ext}(\omega)}{I_{inc}(\omega)} \quad (24)$$

where

$$P_{ext}(\omega) = r_\infty\int_0^{2\pi} d\varphi\mathbf{S}_{ext}(\omega)\cdot\mathbf{r}|_{r=r_\infty} \quad (25)$$

$$\mathbf{S}_{ext}(\omega) = \frac{1}{2}\mathrm{Re}\left[\mathbf{E}_{inc}(\omega)\times\mathbf{H}_{sca}(\omega)^* + \mathbf{E}_{sca}(\omega)\times\mathbf{H}_{inc}(\omega)^*\right] \quad (26)$$

C. *Numerical Details*

Infinite metallic nanowires can be considered as a two-dimensional model. Two-dimensional nature of the problem, allow we use large, dense grid, without too much calculation burden. To assure good convergence, we have actually used $\Delta x = \Delta y = \Delta = 0.1nm$ in all the results presented here. We generally consider grids in x and y ranging from -1000 to 1000 nm, with the silver cylinder structures centered about the origin. But for a single and two nanowires, to shorten the calculation time, we can choose 200 and 400 grid points in each direction. In order to ensure a stable simulation, time steps τ must under the Courant stability limit $\tau_C = \Delta/\left(3^{1/2}c\right)$; however for good convergence we chose to use steps $\tau = \tau_C/2$. 150×10^{-15} s is a good length of time to get accurate Fourier transformed fields.

In order to obtain accurate Fourier-transformed fields necessary for such calculations, incident Gaussian damped sinusoidal pulses were introduced into the computational domains using the total-field scattered-field technique[8].

We do calculations by treating the metal as silver with a Drude plus two-pole Lorentz form for its dielectric constant [9]. We find, $\varepsilon_\infty = 2.3646$, $\omega_D = 8.7377\text{eV}$, $\gamma = 0.07489\text{eV}$, $\Delta\varepsilon_{L1} = 0.3150$, $\omega_{L1} = 4.3802\text{eV}$, $\delta_{L1} = 0.28\text{eV}$, $\Delta\varepsilon_{L2} = 0.8680$, $\omega_{L2} = 5.183\text{eV}$, $\delta_{L2} = 0.5482\text{eV}$ provide a good description of empirical dielectric constant data for silver over the $\lambda = 250\text{nm} - 1000\text{nm}$ range of interest.

III. NUMERICAL CALCULATION MODEL

A. *Isolated Ag Cylinder*

Before studying on the properties of the cylinder surface-plasmon resonance, we should know the accuracy of our FDTD calculations. So we first calculate *TE* scattering off a single Ag cylinder. Then compare with the analytical solution for this case.

Fig.1 displays as curves the analytical cross sections for TE scattering off an Ag cylinder with radius a=25 nm. The symbols in the figure, are now the FDTD cross sections estimated from a single propagation as discussed in Sec. Ⅱ, using the same Drude and plus two-pole Lorentz dielectric constant model. The analytical and FDTD cross sections agree to within 10% or better. Because the FDTD method has been previously used for the calculation of optical scattering cross sections, we believe this is demonstration that the FDTD method can reproduce metal nanowires scattering cross sections with reasonable accuracy.

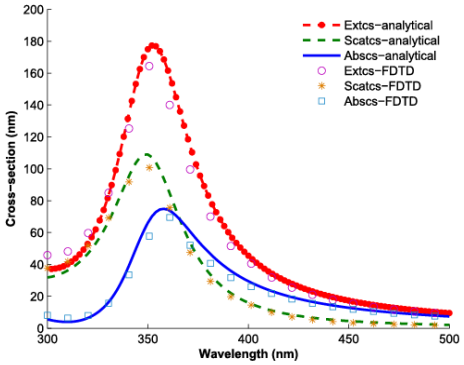

Figure 1. Comparison of analytical (smooth curves) and FDTD-based (symbols) cross sections for a single Ag cylinder of radius a =25 nm. Extcs is short for extinction cross section. Scatcs is short for scattering cross section. Abscs is short for absorption cross section.

The large peaks in Fig.1 are due to the surface Plasmon polarizations(SPP)resonance. FDTD algorithm can adequately reproduce the trends in the cross sections. So we can study on optical properties of nanowires using FDTD.

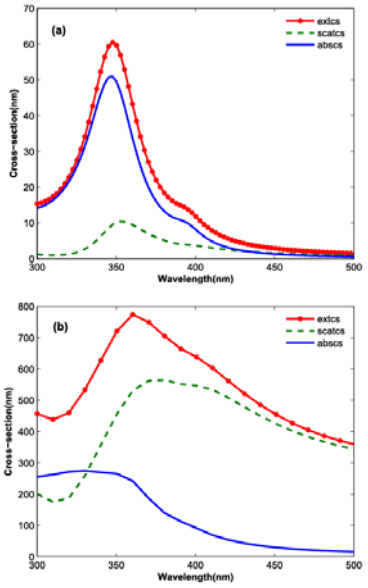

Figure 2. Comparison cross sections for a single Ag cylinder, (a) radius a = 15 nm and (b) radius a = 100 nm.

We study on a single Ag cylinder with different radius using FDTD method. We can see from Fig.2 that, as the cylinder radius a increases, the resonance peak redshifts and broadens, and scattering becomes more dominant than absorption. As radius a = 15 nm, the resonance occurs at $\lambda \approx$ 350 nm and near this wavelength $\sigma_{sca} / \sigma_{abs} \approx 0.2$, absorption is more intense than scattering. When a=100nm the resonance has redshifted to $\lambda \approx 360$ nm with scattering, becoming more pronounced than absorption, $\sigma_{sca} / \sigma_{abs} \approx 2.3$. σ_{sca} increases from 11 to 554 nm between a = 15 and 100 nm, while σ_{abs} increases from 50 to 274 nm over the same a range.

B. *Linear Arrays of Ag Cylinders*

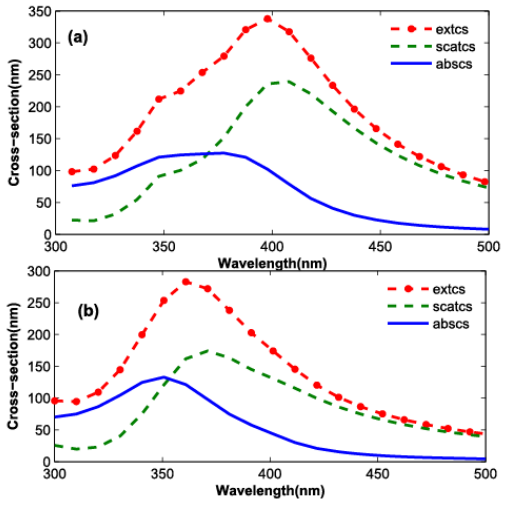

Figure 3. Cross sections for two Ag cylinders (a=25nm). (a) d/a=2.2 and (b) d/a=3

Fig.3(a) presents cross sections for two cylinders. We choose 400 grid points in each direction and centered at the middle of the grid, each with radius a = 25 nm. There is just a

5-nm space between the two cylinders along y, and the ratio of the distance d between their centers and the cylinder radius is d/a = 2.2. The cylinders were exposed to y-polarized light moving from left to right along x. This choice of polarization, given the configuration of the particles, is ideally suited to exciting coupled surface-plasmon resonances consistent with induced (and oscillating) dipoles in each cylinder along the y axis. In particular, we find two structures in the cross sections in the 300–500 nm wavelength region, one a shoulder or weak (λ = 350 nm) close to the single-cylinder surface-plasmon resonance of Fig.1, and stronger maximum redshifted (λ = 400 nm) from the weaker peak. The presence of extra resonance features relative to the single-particle case is due to the interaction of the cylinders at very short separations. Comparable two cylinders calculations but with d/a = 3 in Fig.3(b), shows just one peak and are similar to the single-cylinder results. The nature of the resonance structures in Fig.3 is interesting. Whereas one might naively think the 350 nm structure, owing to its position, is the two-cylinder analog of the single-cylinder dipolar resonance, plots(not shown) of the charge density indicate that it is of mixed dipolar and quadrupolar character, whereas the larger peak to the red of the shoulder is a more of a pure dipolar excitation.

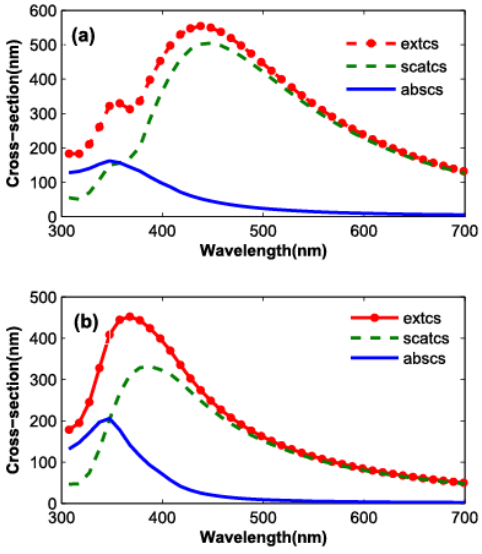

Figure 4. Cross sections for four a=25nm Ag cylinders. (a) d/a=2.2 and (b) d/a=3

Results for a=25 nm and four Ag cylinders are given in Fig.4 for both d/a = 2.2 and d/a = 3. There is a continuation of the pattern for two cylinders in Fig.3. For d/a=2.2 there are two peaks in the 300–500 nm region, with now the smaller peak near 350 nm being better defined and the larger peak being more redshifted from the smaller peak than the two-cylinder result. The width of the larger peak is also larger than the two-cylinder result. As with the two-cylinder result, the d/a = 3 cross sections are simpler and more like the single results, although both the magnitude and widths of the corresponding structures are larger than the single results.

IV. Conclusion

We presented an FDTD approach to studying the interaction of light with nanoscale radius metallic cylinders or nanowires. We obtained reasonably accurate cross sections for single- and multiple-cylinder arrays, confirming the reliability of our approach. There are many directions for future work. It is likely that the intensity of light developing and propagating between the nanowires can be significantly enhanced by varying the distance between the nanowires, cylinder radius, and of course the wavelength and propagation direction of the incident light.

Acknowledgment

This work was supported by the National Natural Science Foundation of China under Grant (Nos. 60931002, 61101064, 51277001, 61201122), DFMEC (No. 20123401110009) and NCET (NCET-12-0596) of China, Distinguished Natural Science Foundation (No.1108085J01), and Universities Natural Science Foundation of Anhui Province (No. KJ2011A002), Graduate Academic Innovate Research Foundation (No.60931002, 61101064), and the 211 Project of Anhui University.

References

[1] K. S. Yee, “Numerical solution of initial boundary value problems involving Maxwell’s equations in isotropic media”, *IEEE Transactions on Antennas and Propagation*, vol.14, 302–307, 1966.

[2] U. Kreibig and M. Vollmer, *Optical Properties of Metal Clusters*, Springer:Berlin, 1995.

[3] C. F. Bohren and D. R. Huffman, *Absorption and Scattering of Light by Small Particles*, Wiley & Sons, Inc.: New York, 1983.

[4] P. B. Johnson and R. W. Christy, “Optical Constants of the Noble Metals”, *Phys. Rev. B*, vol.6, 4370, 1972.

[5] S. K. Gray and T. Kupka, “Propagation of light in metallic nanowire arrays: Finite-difference time-domain studies of silver cylinders”, *Phys. Rev. B*, vol.68, 045415, 2003.

[6] A. D. Boardman, *Electromagnetic Surface Modes*, edited by A. D. Boardman ,Wiley: NewYork, 1982.

[7] A. Taflove and S. C. Hagness, *Computational Electrodynamics: The Finite-Difference Time-Domain Method*, 2nd ed., Artech House, Boston, 2000.

[8] J. M. McMahon, S. K. Gray, and G. C. Schatz, “Nonlocal Optical Response of Metal Nanostructures with Arbitrary Shape ” , *Phys. Rev. Lett*, vol.103, 097403,2009.

[9] T. W. Lee and S. Gray, "Subwavelength light bending by metal slit structures," *Opt. Express*, vol.13, 9652-9659,2005.